Computer simulation of heat affected zone during MIG brazing of zinc-coated steel sheets

P. Sejč[1]*, R. Bielak[2], P. Švec[1], M. Roško[1]

[1] *Strojnícka fakulta STU, Pionierska 15, 831 02 Bratislava, Slovak Republic*
[2] *Institut für Umformtechnik und Hochleistungslasertechnik, Franz Grill Str. 1/345, A-1030 Wien, Austria*

Received 19 April 2006, received in revised form 28 June 2006, accepted 4 July 2006

Abstract

Compared to MAG welding, the main advantage of MIG arc brazing of zinc-coated steel sheets with copper-based filler metal is the resistance of the joint to atmospheric corrosion. However, evaporation of zinc coating can occur in the heat affected zone if an incorrect temperature cycle for brazing is chosen and the joined construction can thus lose its corrosion resistance as a whole. This paper introduces a model which, using finite element method, allows simulation of temperature field progress in the heat affected zone and optimization of MIG brazing parameters for lapped joints. The model was verified by a series of experiments with zinc coated steel sheet FeP05GZ100MB (EN 10 142/90) with thickness of 1.5 mm and filler metal of CuSi3 type.

K e y w o r d s: simulation of heat affected zone, finite element method (FEM), zinc coated steel sheet, arc brazing

1. Introduction

Increased demand for corrosion protection in the automotive industry caused introduction of zinc-coated sheets into production of parts of automobile bodyworks. Main priority of their utilization is a higher possibility of anticorrosion guarantee for the bodywork, which comes from the galvanic protection function of zinc [1]. Under the conditions of electrochemical corrosion, the potential of Zn, which is lower than the one of Fe, ensures its anodic polarization and at the same time also cathodic protection of steel against corrosion. The zinc coating maintains this protective function also to some extent of local disruption [2].

Arc-welding conditions of zinc coated sheets in MAG protective atmosphere are significantly influenced by the existence of metal coating [3]. Zinc is characterized by relatively low melting and evaporation temperature: 420 ℃ and 906 ℃, respectively (Table 1). Both these temperatures are lower than temperatures commonly used for fusion welding of steel sheets. Hence the arc welding of zinc coated sheets is accompanied by intensive evaporation of zinc coating from the material surface, which influences not only the welding process, but also the joint quality [4].

Another disadvantage of MAG arc welding when using a steel wire, e.g. G2Si (Table 2), is the loss of corrosion resistance in the joint. The joint and the heat affected zone can be additionally treated by zinc sprays, but the level of protection is lower and the production costs are increased.

More advantageous is using a copper-based filler metal. This filler metal ensures continuity of corrosion resistance at corresponding strength and other mechanical properties of the joint.

From the practical point of view, CuSi3, CuAl8 and CuSn6 alloys are most suitable as filler metal for joining of zinc coated sheets made of unalloyed steel [7, 8, 11]. Based on their composition, these wires have different fluidity, but provide also different strength and hardness of the joint (Table 3). Because of their high Cu content, these materials have a relatively low melting temperature (875 ℃ to 1040 ℃). During application of melted metal, the base material is only wetted without being melted, with minimal melting of the sheet edge – hence this technology is referred to as MIG brazing in practice.

*Corresponding author: tel.: +421 2 44455086342; fax: +421 2 44455086; e-mail address: pavol.sejc@stuba.sk

Table 1. Selected physical properties of Fe and Zn [5]

	Melting temperature (°C)	Evaporation temperature (°C)	Ionizing energy $M^+ + e$ (eV)	Specific electric conductivity at 0 °C ($MS \cdot m^{-1}$)
Fe	1535	3000	7.87	11.5
Zn	419.5	906	9.39	21.7

Table 2. Typical chemical composition of G2SI wire (EN 440 standard) [6]

Element content in %			
Fe	C	Si	Mn
the rest	0.10	0.60	1.10

To minimize the negative influence of Zn vapors on the stability of arc burning and metal transfer during MIG brazing, it is important to ensure low overheating of base material. The material, however, cannot be cold and must be heated minimally to the working temperature. Minimal brazing temperature depends on the type of joint [10]:

– during building up brazing, when the brazed areas are only wetted by the liquid filler metal, heating temperature of the base material should be 50–200 °C lower than solidus of the filler metal,

– during capillary brazing the brazing filler metal is required to leak into the joint, hence the base material must be heated to a higher temperature: usually 20–100 °C above solidus of the filler metal.

Introduction of correct heat amount is important also from the point of view of maintaining the amount and quality of protective coating needed for corrosion resistance of the heat affected zone. The cathodic effect of Zn only affects a short distance (1 to 2 mm [2]) when the coating is disrupted. In case of more severe damage, such as evaporation of zinc from the heat affected zone, there is a risk of a quick corrosion damage to the uncovered area. This way, the main advantage of MIG brazing over MAG welding can be lost and the introduction of a more expensive Cu-based filler metal becomes questionable.

2. Modelling of MIG brazing

The aim of FEM analysis was to determine the temperature and temperature fields distribution during MIG brazing. For this purpose, a model with geometry shown in Fig. 1 was designed.

The dimensions of the model correspond to real dimensions of specimens used for practical experiments.

As seen in Fig. 1, two sheets were joined using a lapped joint, the upper sheet being 70 mm wide and the lower one with width of 140 mm. The length of the joint was 150 mm. Exact position of the sheets was ensured by a clamping device. A simplified shape was used for the geometry of the brazing filler metal. This shape was created by rectilinear movement of a spherical cap in the direction of brazing. The volume of the filler metal was the intersection of this spherical cap and the joined sheets of prismatic shape, as seen from the cross-section and from the top view in Figs. 1–3. Dimensions of the brazing filler metal were determined by the radius of the spherical cap R (Fig. 1). This radius was chosen so that the width (b) and height (h) of the simulated joint are identical with the average dimensions measured on real specimens. These dimensions are influenced by the welding parameters, especially by the welding speed. Geometry of filler metal depends also on the stability of the process. During computation, the gradual addition of spherical filler metal, corresponding to individual time steps of the simulation was modelled.

Thermal analysis of brazed specimens was per-

Table 3. Chemical composition and selected properties of brazing wires [9]

Wire designation according to DIN 1733	Chemical composition (%)						Melting temperature (°C)	Mechanical properties			
	Cu	Si	Sn	Al	Mn	P		R_m ($N \cdot mm^{-2}$)	Brinell hardness HB 2.5/62.5	Elongation (%)	Notched bar impact work (J)
SG CuSi3	Balance	2.9	–	–	0.9	–	965–1035	350	80	40	60
SG CuAl8	Balance	–	–	8.0		–	1030–1040	430	100	40	100
SG CuSn6	Balance	–	8.0	–	–	0.1	875–1025	260	80	20	32

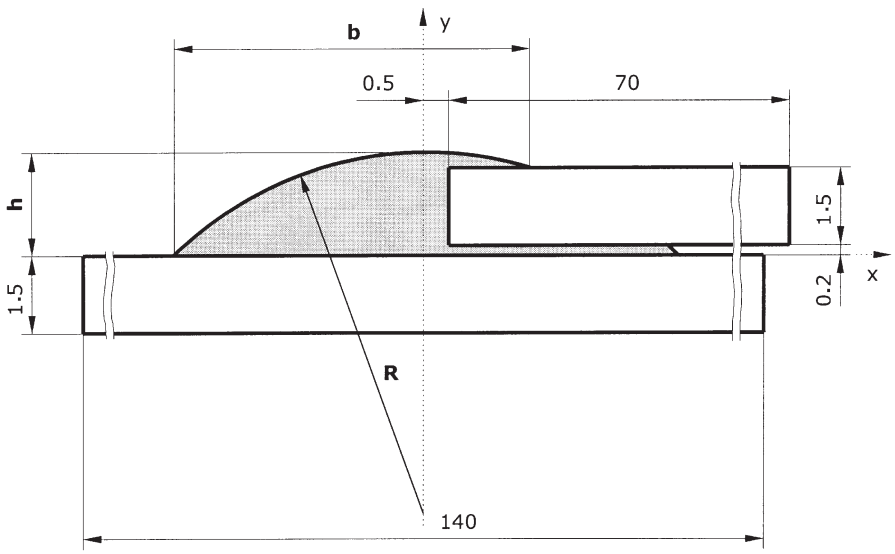

Fig. 1. Geometry of the model used for MIG brazing simulation, front view.

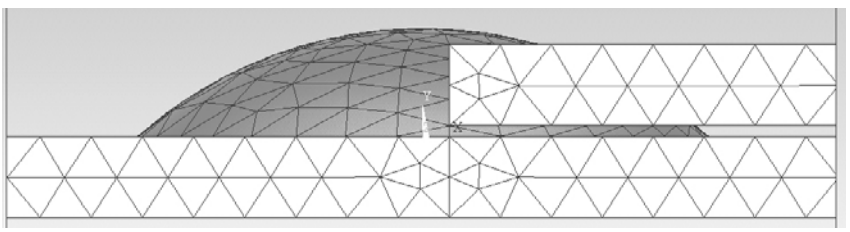

Fig. 2. Cross-section of the model with meshing shown in the area of joint.

formed using ANSYS software, which utilizes the principles of finite element method. In this software product, thermal processes for isotropic material are generally described by Fourier's equation (1) of non-stationary temperature field [12]:

$$\frac{\partial T^2}{\partial x^2} + \frac{\partial T^2}{\partial y^2} + \frac{\partial T^2}{\partial z^2} + \bar{q} = \frac{\rho \cdot c}{\lambda} \frac{\partial T}{\partial t}, \qquad (1)$$

where $\bar{q}$ is the capacity of heat source, T is temperature, t is time, ρ is density, c is specific heat and λ is coefficient of thermal conductivity.

Temperature dependences of thermophysical properties of the model, such as density, specific heat and coefficient of thermal conductivity, were entered into the simulation. The material properties were obtained from literature [13] and are given in Tables 4 and 5.

The geometrical model, in accordance with the finite element method, was divided into volumetric elements with 8 nodes (Figs. 2 and 3). Finer mesh was chosen in the area of the joint (Fig. 3), which increased the accuracy of the computation in this location.

Constant temperature distribution of 20 °C throughout the whole volume of the specimen was taken as initial condition before the start of the process. The

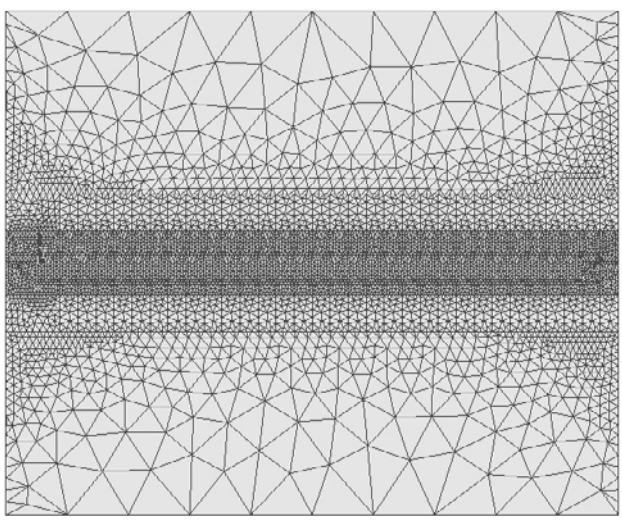

Fig. 3. Mesh of the entire model, top view.

simulation consisted of non-stationary thermal analysis of the specimen. The heat flow was positioned onto the area of the brazing filler metal using boundary condition of 2nd order, applying Gauss distribution

Table 4. Thermophysical properties of steel [13]

T (°C)	20	400	600	720	800	876	900	1000	1200	1450	1476	1523	1550	1800
ρ (kg·m^{-3})	7802	7691	7637	7606	7589	7567	7561	7536	7486	7425	7420	7406	7399	7335
C_p (J·kg^{-1}·K^{-1})	436	515	567	690	720	760	760	705	710	714	8264	8264	730	730
λ (W·m^{-1}·K^{-1})	45	39.2	34.7	32	31.9	31.7	31.5	31.4	33.1	140	145	155	160	170

Table 5. Thermophysical properties of the brazing filler metal [13]

T (°C)	20	400	600	720	800
ρ (kg·m^{-3})	8960	8783	8697	8623	8613
C_p (J·kg^{-1}·K^{-1})	382	400	415	420	422
λ (W·m^{-1}·K^{-1})	391	356	344	335	331

Table 6. Heat transfer coefficient [13]

T (°C)	20	500	720	780	1000	1440	1500	2862	3000
h_c (W·m^{-2}·K^{-1})	9.80	50.25	77.54	85.76	141.10	306.76	331.45	891.91	948.70

of heat flow density according to Eq. (2):

$$q(r) = \sqrt{\frac{1}{2 \cdot \pi}} \cdot q_S \cdot e^{-\frac{r^2}{2}}, \qquad (2)$$

where $q(r)$ is the heat brought in, q_S is planar heat density and r is radius.

The source diameter was 2 mm, its axis of action being in the middle of coordinate system with a 20° inclination with respect to the vertical axis of the joint. The cooling of specimen's free surface to the ambient temperature of 20 °C was simulated using a boundary condition of 3rd order with surface heat transfer coefficient given in Table 6.

The simulation of temperature fields on the bottom side of lapped joint was performed at different values of specific heat input. The changes of heat input were achieved by changing the velocity of the heat source only, according to Eq. (3):

$$Q = \frac{U \cdot I}{v}, \qquad (3)$$

where U is the voltage in the arc, I is current and v is brazing velocity.

Input brazing velocities were v = 350, 400, 450 a 500 mm·min^{-1}, resulting in specific heat input Q = 219.5; 212.2; 169.7 and 153.4 kJ·m^{-1}, respectively.

3. Experiment

Experimental verification of the simulation output took place on specimens made of double-sided zinc coated steel FeP05GZ100MB (EN 10 142/90) with thickness of 1.5 mm. The properties and chemical composition of the base material are given in Table 7.

Table 7. Basic properties of sheet metal used for production of specimens (atest)

Chemical composition	Mechanical properties
C = 0.06 % max.	R_e = 140 ÷ 260 MPa
Mn = 0.35 % max.	R_m = 270 ÷ 380 MPa
P = 0.025 % max.	A_{80} = 30 % min.
S = 0.025 % max.	Thickness of Zn-layer: 6 ÷ 12 μm

Table 8. Chemical composition and selected properties of filler metal CuSi3 [6]

Chemical composition	Mechanical properties
Si = 2.8 ÷ 4.0 %	R_e = min. 147 MPa
Sn = max. 0.2 %	R_m = min. 392 MPa
Zn = max. 0.2 %	A = 46 % min.
Mn = 0.5 ÷ 1.5 %	HB = 85 ÷ 100
Fe = max. 0.3 %	$T_{melting}$ = 910 ÷ 1025 °C
Cu = the rest	Positions according to STN EN 287: PA, PB, PC, PD, PF

An SG CuSi3 wire with diameter d = 1 mm was used as filler metal. Its chemical composition and selected properties are shown in Table 8.

The brazing was performed using welding power supply HOBART ARC – MASTER 501 with wire feed

unit Hobart Ultrafeed 1000. Torch travel was mechanized using modified cutting tractor RS 13. This assembly allowed to set a constant brazing velocity up to 600 mm·min^{-1} and to adjust the geometry of torch movement – the angle of torch inclination with respect to the sheet plane and to the wire extension. The specimens were brazed in protective Ar-atmosphere, the flow rate was set to 15 l·min^{-1}. The brazing took place at average current value $I = 67$ A and average voltage $U = 19$ V.

For measurement of temperature conditions in the heat affected zone (HAZ) on the bottom side of the lapped joint, the workplace was equipped with a PC with measurement card PCL 818, to which two thermocouples of chromel-alumel type (T1, T2) were connected (Fig. 4).

The thermocouples were positioned at a distance of 50 and 100 mm from the starting brazing location, i.e. in 1/3 and 2/3 of the specimen.

The amount of input heat was controlled by changing of torch movement velocity.

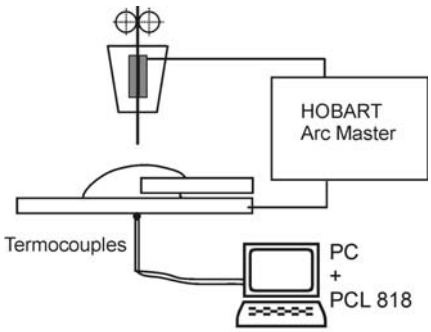

Fig. 4. Diagram of temperature measuring in HAZ.

4. Results

The simulation output for given brazing velocities provided information on temperature fields distribution in individual specimens. The temperature progress on the surface of joined sheets in the time steps of brazing and for given parameters was examined especially with the aim to find locations with maximum temperature and to compare the recorded temperatures with the evaporation temperature of zinc (906 ℃).

The results, obtained for all brazing velocities, showed that the maximum temperature on the surface of base material, which is critical for anticorrosion function of zinc coating, was located on the bottom side in the axis of the joint. This corresponds to the axis of heat source used in the simulation. Lowering the brazing velocity increased not only the temperature, but also the width of area, in which the evaporation temperature of zinc was exceeded. In all cases there was a start stage, characterized by temperature growth, after which there was a stabilization of

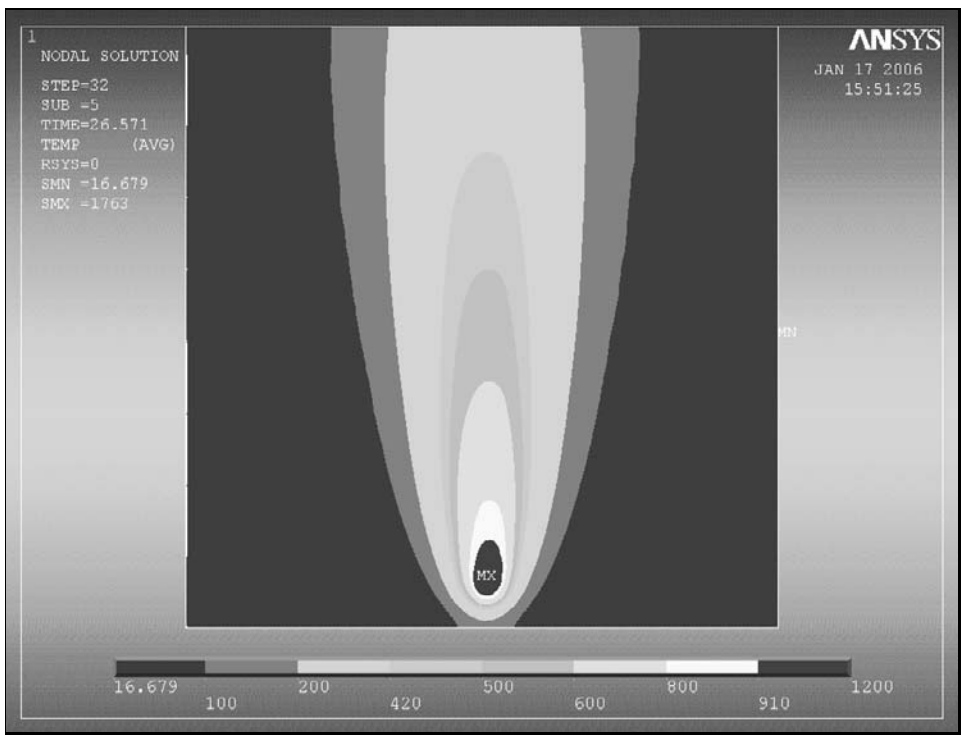

Fig. 5. Temperature field distribution at the quasi-stationary state, brazing velocity $v = 350$ mm·min^{-1}.

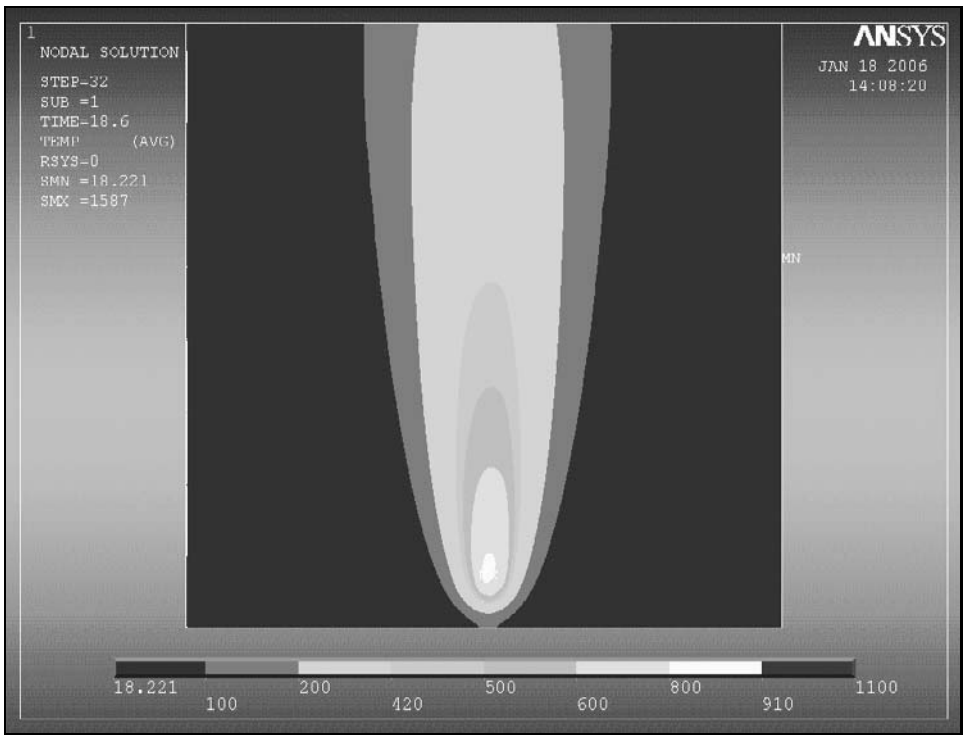

Fig. 6. Temperature fields distribution at the quasi-stationary state, brazing velocity $v = 500$ mm/$\cdot$min^{-1}.

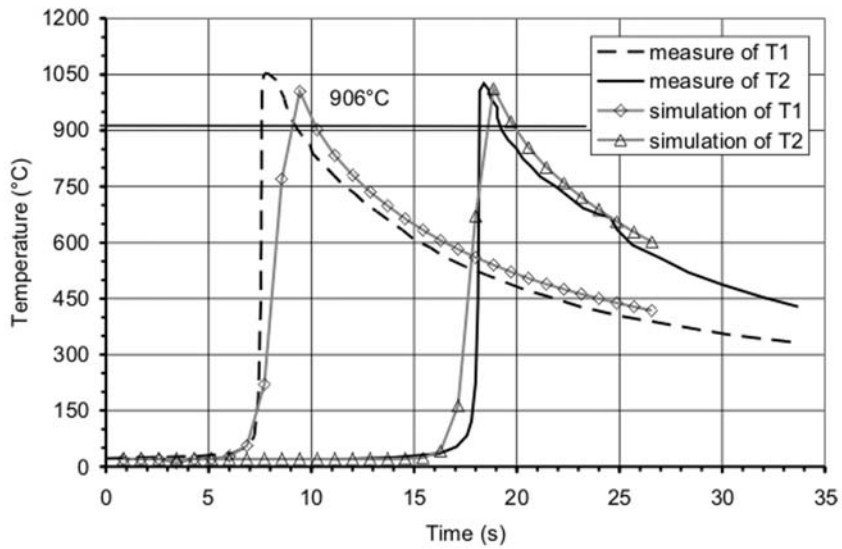

Fig. 7. Temperature cycles of brazing, brazing velocity v = 350 mm$\cdot$min^{-1}.

the temperature progress, characterized by a relatively small change of temperature in two consecutive steps. This quasi-stationary state is important for real process and was achieved in a distance of approximately 40 mm from the start point of brazing. Attention was aimed mainly to the results obtained after exceeding this limit.

Next experiment was to compare the time progress of temperature measured during real brazing of specimens and the one obtained from the simulation at equal parameters. The measurement was performed in the location of maximum temperature in the axis of the joint, in 1/3 and 2/3 of the specimen length.

Examples of the temperature field distribution at the quasi-stationary state, on the bottom side of the lapped joint for minimal and maximal chosen brazing velocity are shown in Figs. 5 and 6. Figures 7 and 8 show the time progress of temperatures obtained from the simulation and measured on real specimens.

It can be seen, that at the lowest chosen brazing

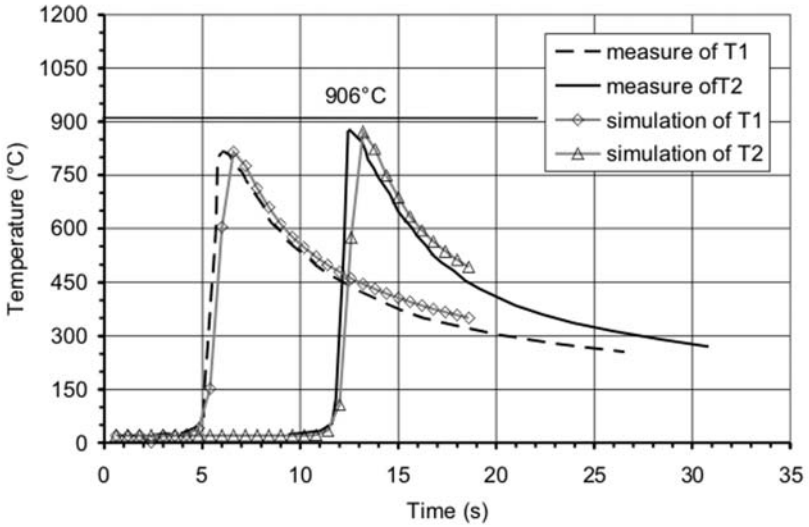

Fig. 8. Temperature cycles of brazing, brazing velocity $v = 500$ mm·min^{-1}.

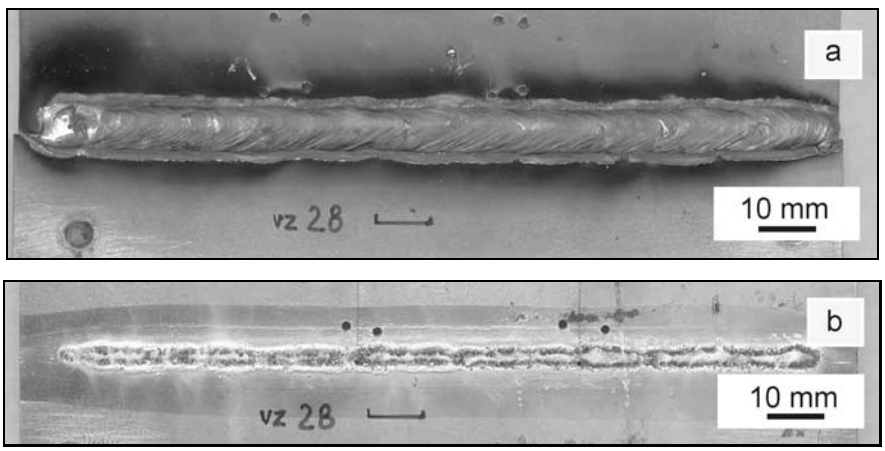

Fig. 9. Topography of the brazed joint surface, brazing velocity $v = 350$ mm·min^{-1}: a) upper side, b) lower side.

velocity $v = 350$ mm·min^{-1}, i.e. at the highest heat input $Q = 219.5$ kJ·m^{-1}, the temperature on the sheet surface in HAZ reached its maximum value ($T_{\max}$), which exceeds the temperature of zinc evaporation (906 ℃). This temperature was exceeded in a 6 mm wide area. Based on the simulation we can assume, that evaporation of protective layer from the surface of the steel sheet will occur in an area bounded by isothermal line with $T = 906$ ℃. However, from the point of view of corrosion resistance as a whole it is important, that no destruction of Zn protective layer in HAZ occurs, or that the area of destruction is minimal to ensure at least cathodic protection of the base steel sheet.

The simulation output was verified on real specimens prepared at the same parameters, where a continuous, 3–5 mm wide area of disrupted Zn protective layer was identified. This area is shown in Fig. 9b, showing the extent of damage on a joint, prepared at $v = 350$ mm·min^{-1}. In Fig. 9a, the upper side of the joint is characterized by a uniform surface of the bead.

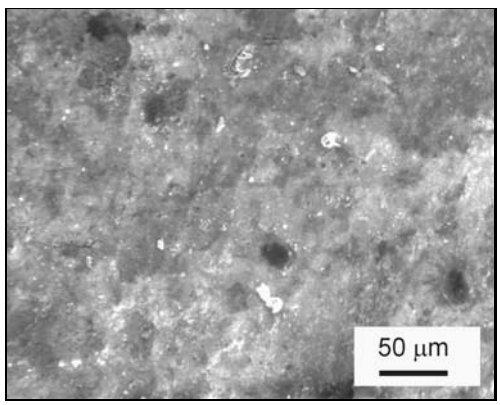

Fig. 10. Compact zinc layer without heat affection, SEM.

Qualitative change of protective layer disruption, depending on the brazing temperature achieved, is shown in Figs. 10–12. Figure 10 shows the sheet sur-

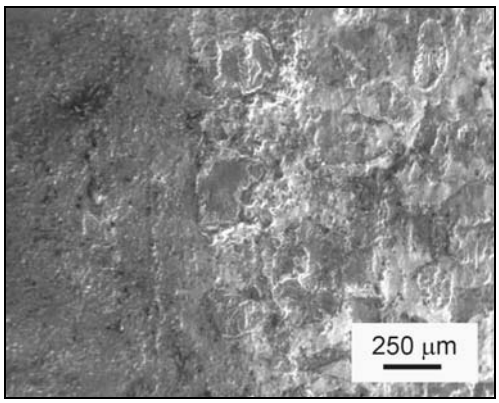

Fig. 11. Surface with temperature between the melting temperature and evaporation temperature of zinc, SEM.

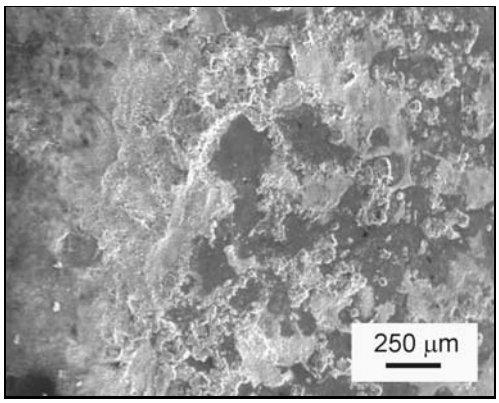

Fig. 12. Interface of the surface with temperature higher than the evaporation temperature of zinc, SEM.

face without heat affection, with a compact protective Zn coating. Local porosity does not have a negative influence on the anticorrosion protection. Specimen surface from an area, where the melting temperature of zinc has been exceeded, but its evaporation temperature has not yet been reached, is shown in Fig. 11. A compact zinc layer with minimal damage is maintained on the surface. This damage is characterized by generation of white areas, representing an oxidation damage of zinc layer, confirmed in [14, 15]. Figure 12 shows a transitional area between a compact layer and surface without protective Zn coating. Places with evaporated zinc are evident. Areas, covered with an oxidic film, can be seen as well.

From the results it can be assumed, that a heat affected zone with this extent of damage of protective Zn layer is no more able to ensure corrosion resistance of the uncovered surface. In this case, the significant advantage of MIG brazing is being lost, as this method requires more expensive filler metal compared to MAG welding with a steel wire.

At the highest brazing velocity $v = 500\ \mathrm{mm \cdot min^{-1}}$ and at the lowest heat input $Q = 153.4\ \mathrm{kJ \cdot m^{-1}}$, the simulated temperature on the sheet surface in HAZ did not reach the evaporation temperature of zinc (Figs. 6 and 8), which was verified also experimentally on real specimens (Fig. 13b). The HAZ was hence showing no significant destruction of Zn protective layer, there was only a local layer disruption, which did not exceed the cathodic protection limit. However, critical parameter at high brazing velocity was the arc burning stability, which was negatively influenced by vaporizing zinc, released from the surface of the material. Higher pressure of Zn vapors, acting against the direction of the melted metal drop from the end of electrode, through the arc and towards the base material, caused a bead with non-uniform width and with metal spatter, as seen in Fig. 13a. Another difference was a significantly faster cooling of the brazing filler metal, which can be seen in Fig. 8 as a steeper cooling phase on the temperature cycle curve. Lower solidification and cooling time can cause insufficient

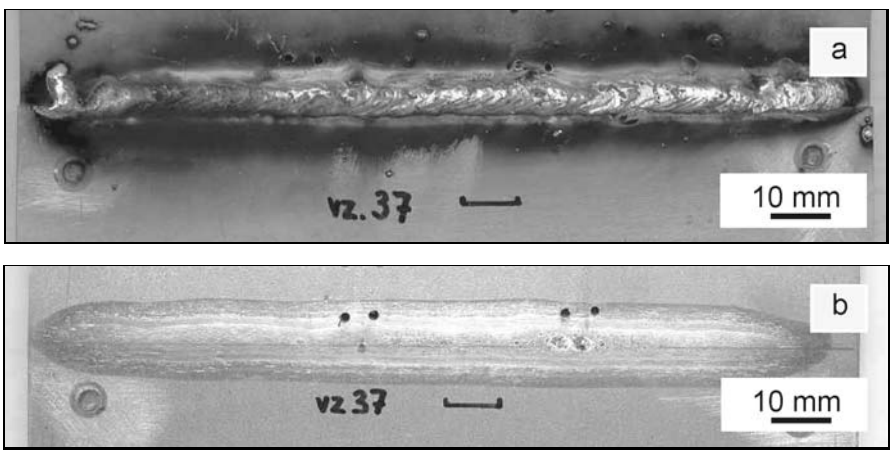

Fig. 13. Topography of the brazed joint surface, brazing velocity $v = 500\ \mathrm{mm \cdot min^{-1}}$: a) upper side, b) lower side.

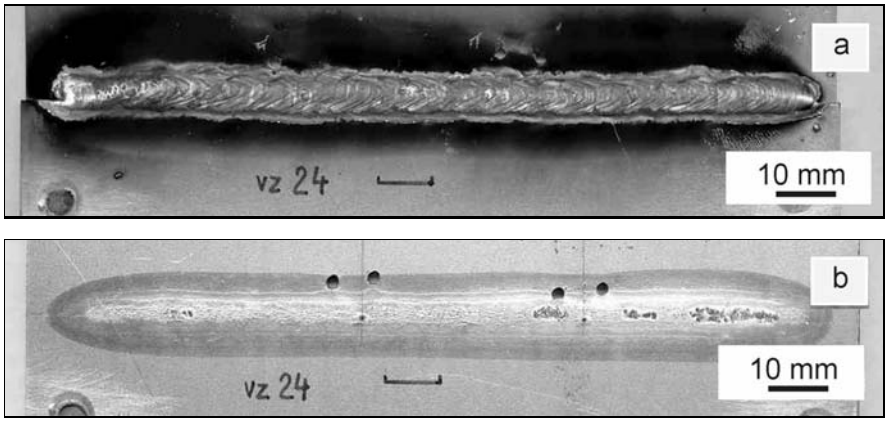

Fig. 14. Topography of the brazed joint surface, brazing velocity $v = 450$ mm·min^{-1}: a) upper side, b) lower side.

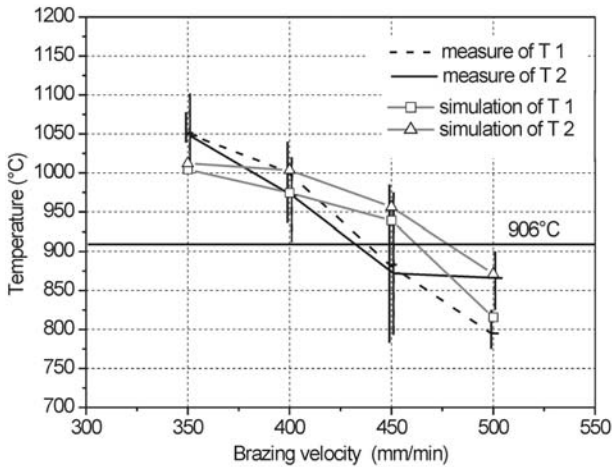

Fig. 15. The influence of brazing velocity on maximum temperature on the bottom side of HAZ: T_1 – thermocouple located in 1/3 of the joint length, T_2 – thermocouple located in 2/3 of the joint length.

degassing of welding point, which can result in defects in the joint, such as gas inclusions and pores [4]. Defects of this character significantly decrease the active cross-section of the joint and decrease thus also its strength.

As a result of examination of the MIG brazing process, brazing velocity $v = 450$ mm·min^{-1} was determined to be optimal, with its corresponding heat input $Q = 169.7$ kJ·m^{-1}. This value ensures a uniform bead, as well as preservation of protective coating on real specimens, as seen in Fig. 14. The uniform bead of the applied filler metal, without metal spatter confirms good arc burning stability and metal transport from the electrode to the welding point. Preservation of compact Zn layer in HAZ on the bottom side of the joint confirms the preservation of functionality of protective Zn layer also in the heat affected zone.

Comparison of the maximum temperatures computed in the simulation and the maximum temperatures measured during the experiments in the points of thermocouple location is shown in Fig. 15 for all chosen brazing velocities. There is a variance of the measured values, which corresponds to the results of several experiments. The simulated temperatures never exceeded this measured interval.

5. Conclusion

The aim of the presented paper was a design of a simulation model for heat affection of the base material during arc MIG brazing of zinc-coated steel sheets. The model for finite element method was tested using ANSYS software and verified by a series of practical experiments, during which lapped joints were created on a FeP05GZ100MB sheet (EN 10 142/90) with width of 1.5 mm. CuSi3 wire of 1 mm diameter was used as filler metal. The brazing was performed in Ar protective gas, brazing velocities were $v = 350$, 400, 450 and 500 mm·min^{-1}. Change of the velocity affected the heat input, which has a direct influence on the measured surface temperature $T_{\max}$, extent of heat affection and also on the character of Zn layer damage.

It follows from the simulation output, that the critical area from the point of view of maintaining a compact Zn layer (thus maintaining the corrosion resistance of the construction) is the bottom side of the lapped joint. Using the lowest brazing velocity $v = 350$ mm·min^{-1} and thus the highest heat input $Q = 219.5$ kJ·m^{-1}, the temperature on the surface exceeded the evaporation temperature of zinc (906 ℃) in a width of 6 mm. These results correspond to the values measured on real specimens, where the width of evaporated zinc layer was ranging from 3 to 5 mm. Both of these values exceed the extent of damage, where the cathodic function of Zn coating is acting.

Using the highest brazing velocity $v = 500$ mm·min^{-1} and lowest heat input $Q = 153.4$ kJ·m^{-1}, the surface temperature in the measured area was lower

than the evaporation temperature of zinc. This was also confirmed on the real specimens, where no destruction of Zn coating in HAZ was observed. However, higher brazing velocity decreased the stability of arc burning (negative influence of Zn vapors during fast evaporation of the coating), which caused a non-uniform bead width and resulted in pores and gas inclusions in the joint.

Using the new MIG brazing model, the brazing velocity, along with the corresponding heat input was optimized. For the base and filler material and for the type of joint used in the experiments, the brazing velocity $v = 450\ \mathrm{mm \cdot min^{-1}}$ was determined as optimal. This velocity was verified on a real specimen, resulting in a uniform bead (confirming arc burning stability and metal transfer) with minimal local disruption of the protective Zn layer, preserving its protective function in the heat affected zone.

Acknowledgements

The results presented in this paper were achieved as a part of VEGA grant No. 1/2086/05.

References

[1] MARDER, A. R.: Progress in Material Science, *45*, 2000, p. 191.
[2] HACKL, H.: Welding Review International, November 1996, p. 122.
[3] LIVELL, G.—LANGILL, T.: PCI Journal, May–June 1998, p. 40.
[4] DITHEY, U.—REISGEN, U.—DICKERSBACH, J. —WARMUTH, P.: Schweissen und Schneiden, *52*, 2000, p. 660.
[5] GAŽO, J.: Všeobecná anorganická chémia. Bratislava, ALFA 1978.
[6] ESAB – Katalóg prídavných zváracích materiálov a zariadení, 2004, CD.
[7] FRINGS, A.: Schweissen und Schneiden, *38*, 1986, p. 624.
[8] DITHEY, U.—HOECKER, F.: Welding in the World, July 2004, p. 31.
[9] BEDRA – Wire, solutions for welding technology. www.berkenhoff.de
[10] RUŽA, V.: Pájení. Praha, SNTL 1978.
[11] FRINGS, A.—STÖCKEL, S.: Schweissen & Schneiden, *38*, 1986, p. 624.
[12] BENČA, Š.: Výpočtové postupy MKP pri riešení lineárnych úloh mechaniky. Bratislava, Vydavateľstvo STU 2004.
[13] KRAVÁRIKOVÁ, H.—KOVAČÓCY, P.: Zváranie – Svařování, *50*, 2001, p. 240.
[14] ŠVEC, P.—SEJČ, P.: Acta Mechanica Slovaca, 2-B/2004, p. 437.
[15] SEJČ, P.: Zváranie – Svařování, *52*, 2003, p. 22.